
Learning of Discrete Graphical Models with Neural Networks

Abhijith J.¹, Andrey Y. Lokhov², Sidhant Misra², and Marc Vuffray²

¹ Centre for High Energy Physics, Indian Institute of Science, Bengaluru 560012, India.

² Theoretical Division, Los Alamos National Laboratory, Los Alamos, NM 87545, USA.

Abstract

Graphical models are widely used in science to represent joint probability distributions with an underlying conditional dependence structure. The inverse problem of learning a discrete graphical model given i.i.d samples from its joint distribution can be solved with near-optimal sample complexity using a convex optimization method known as Generalized Regularized Interaction Screening Estimator (GRISE). But the computational cost of GRISE becomes prohibitive when the energy function of the true graphical model has higher order terms. We introduce NeurISE, a neural net based algorithm for graphical model learning, to tackle this limitation of GRISE. We use neural nets as function approximators in an Interaction Screening objective function. The optimization of this objective then produces a neural-net representation for the conditionals of the graphical model. NeurISE algorithm is seen to be a better alternative to GRISE when the energy function of the true model has a high order with a high degree of symmetry. In these cases NeurISE is able to find the correct parsimonious representation for the conditionals without being fed any prior information about the true model. NeurISE can also be used to learn the underlying structure of the true model with some simple modifications to its training procedure. In addition, we also show a variant of NeurISE that can be used to learn a neural net representation for the full energy function of the true model.

1 Introduction

Joint probability distributions of random variables with underlying conditional dependence structure are ubiquitous in science and engineering. The dependency structure of these distributions often reflect the properties of the scientific models that generate them. Undirected graphical models, also known as Markov random fields, are a natural way to represent such distributions and have found use in myriad fields such as physics [5], artificial intelligence [31], and biology [23] to name a few.

Due to the importance of graphical models, the inverse problem of learning them given i.i.d samples from their joint distribution has been a very active area of research. This problem was first addressed by Chow and Liu [8], who solved it for the case of graphical models with a tree structure. Since then there have been many works on learning graphical models under certain assumptions about the true model, with most of them focused on the special case of learning Ising models [28, 18, 26]. Bresler [4] gave the first polynomial time greedy algorithm that learned Ising models without any underlying assumptions. But the number of samples required to learn the model (i.e. sample complexity) using this method was still sub-optimal. The first near-sample optimal method to learn binary models with second order interactions (Ising models) was introduced by Vuffray *et al.* [29]. Under this

¹ abhijithj@iisc.ac.in

² { lokhov, sidhant, vuffray }@lanl.gov

approach, the learning problem is converted to a convex optimization problem which reconstructs the neighborhood of each variable in the model. The generalization of this method to learn any discrete graphical model is known as the *Generalized Regularized Interaction Screening Estimator* (GRISE) [30]. This algorithm runs in polynomial time in the size of the model and its sample complexity is close to known information-theoretic lower bounds [27].

Despite being near sample optimal, the computational cost of GRISE becomes very high when trying to learn models with higher order interactions. To learn a model that has interactions up to order L , GRISE will need to have all possible models at that order in its hypothesis space. For a p variable model with L -order interactions the computation complexity of GRISE goes as $\tilde{O}(p^L)$, which can be high for large L . Even if the true model has a high degree of symmetry or structure that reduces the effective number of parameters to be learned, GRISE will not be able to leverage this in a significant way to reduce the size of its hypothesis space.

In this work we propose a way to overcome this shortcoming arising from the linear parameterization that GRISE uses to represent candidate models. We introduce a method, which we call *Neural Interaction Screening Estimator* (NeurISE), that elegantly combines the strength of GRISE and the non-linear representation power of neural networks. As neural nets are universal function approximators [1, 17], NeurISE has the ability to learn the true model given enough samples just like GRISE. In addition, we demonstrate experimentally that NeurISE is much more efficient than GRISE for learning higher order models with some form of underlying symmetry. We exhibit practical examples where this performance gain can be exponentially large with a parameter space reduction of 99.4% already on small systems of only 7 variables. Another important aspect of graphical model learning is learning the structure of the conditional independence relations between random variables. While one may think at first that the use of a neural network could obfuscate the graphical model structure, we show that with a proper regularization process, the Markov random field structure reappears within the weights of the neural network. Finally, we also provide an aggregated cost function for learning a global probability distribution or energy function using consensus of local NeurISE reconstructions.

Throughout this work we will compare NeurISE to GRISE as it is the current state of the art method for learning undirected discrete graphical models, both theoretically from a sample complexity point of view [30] and empirically [22] when compared to other methods. Other existing recent methods for learning undirected graphical models include greedy [16] and pseudo-likelihood [20, 22, 32] type approaches. On the directed graphical models side, one can mention Directed Acyclic Graph (DAG) based methods that are popular for structure learning in the continuous variable setting [21]. Such methods are not directly related to this work as we are specifically interested in learning the discrete graphical model from which our samples are drawn that is undirected and may have an arbitrary underlying graph structure. Finally, other related line of work deals with testing in graphical models [10, 2] and estimations from single samples [7, 3, 11, 15, 9, 12].

The paper is organized as follows. The interaction screening principle is explained in Section 2 and NeurISE is presented in Section 3. Structure learning with NeurISE using an appropriate initialization and ℓ_1 regularization is illustrated in Section 4. The method for representing the energy function of the true model with a single neural net representation for the energy function is discussed in Section 5. The supplementary material contains additional experimental results with NeurISE.

2 Learning graphical models via interaction screening

2.1 The interaction screening method

We consider a graphical model defined over p discrete variables $\sigma_i \in [q]$ for $i \in [p]$, where the notation $[k]$ refers to the set containing exactly $k \in \mathbb{N}$ elements. The models we consider will be positive probability distributions over the set of p dimensional vectors, $\underline{\sigma} \in [q]^p$. Without loss of generality this probability distribution can be written as,

$$\mu(\underline{\sigma}) = \frac{1}{Z} \exp(H(\underline{\sigma})). \tag{1}$$

The function, $H : [q]^p \rightarrow \mathbb{R}$, is called the *energy function* or the *Hamiltonian* of the graphical model. The quantity Z is called the partition function and it ensures normalization. GRISE considers a linear

parameterization of $H(\underline{\sigma})$ by expanding it with respect to a chosen basis

$$H(\underline{\sigma}) = \sum_{k \in \mathcal{K}} \theta_k^* g_k(\underline{\sigma}_k), \quad (2)$$

where g_k denote the elements of the basis, \mathcal{K} denotes the index set of the basis functions acting on the variables $\underline{\sigma}_k \subseteq \underline{\sigma}$, and θ_k^* are the parameters of the model. Given n i.i.d. samples $\underline{\sigma}^{(1)}, \dots, \underline{\sigma}^{(n)}$, GRISE uses the convex *interaction screening objective* (ISO) to estimate the parameters $\underline{\theta}^*$ around one variable at a time. For any $u \in [p]$, the ISO is given by

$$\text{ISO: } \mathcal{S}_n(\underline{\theta}_u) = \frac{1}{n} \sum_{t=1}^n \exp \left(- \sum_{k \in \mathcal{K}_u} \theta_k g_k(\underline{\sigma}_k^{(t)}) \right), \quad (3)$$

where $\mathcal{K}_u = \{k \in \mathcal{K} \mid \sigma_u \in \underline{\sigma}_k\}$ and $\underline{\theta}_u$ are the parameters associated with \mathcal{K}_u . The quantity

$$H_u(\underline{\sigma}) = \sum_{k \in \mathcal{K}_u} \theta_k g_k(\underline{\sigma}_k) \quad (4)$$

denotes the *partial energy function* containing all terms dependent on σ_u and is directly related to the conditional distribution $\mu(\sigma_u \mid \underline{\sigma}_{\setminus u})$. In the presence of prior information in the form of an ℓ_1 -bound on the parameters, the estimation can be efficiently performed by:

$$\text{GRISE: } \min_{\underline{\theta}_u} \mathcal{S}_n(\underline{\theta}_u), \quad \text{subject to: } \|\underline{\theta}_u\|_1 \leq \gamma. \quad (5)$$

The basis functions in (5) are assumed to be centered: $\sum_{\sigma_u} g_k(\underline{\sigma}_k) = 0$ for all $k \in \mathcal{K}_u$. A quick intuition behind the minimization in (5) can be obtained by considering the ISO in the limit $n \rightarrow \infty$

$$\lim_{n \rightarrow \infty} \mathcal{S}_n(\underline{\theta}_u) \rightarrow \mathcal{S}(\underline{\theta}_u) = \mathbb{E} \left[\exp \left(- \sum_{k \in \mathcal{K}_u} \theta_k g_k(\underline{\sigma}_k) \right) \right]. \quad (6)$$

It is easy to verify using simple computation that $\nabla_{\theta_k} \mathcal{S}(\underline{\theta}_u^*) = 0$. Since \mathcal{S} is a convex function, the minimization in (5) estimates the parameters correctly in the limit of infinite samples. We refer the reader to [30] for a detailed finite sample analysis of GRISE.

2.2 Basis function hierarchies

The choice of basis functions in (3) plays a crucial role in the computational complexity of GRISE. Unless clearly specified by the application, one must use generic complete hierarchies of basis functions that have the ability to express any discrete function $H(\underline{\sigma})$. We present two such generic hierarchies below.

Centered indicator basis: This basis is defined by using the one-dimensional centered indicator functions given by

$$\Phi_s(\sigma) = \begin{cases} 1 - \frac{1}{q}, & \text{if } s = \sigma, \\ -\frac{1}{q}, & \text{otherwise.} \end{cases} \quad (7)$$

For any $\mathcal{K} \subset 2^{[p]}$ a set of basis functions can be constructed as

$$\Phi_{\underline{s}_k}(\underline{\sigma}_k) = \prod_{i \in k} \Phi_{s_i}(\sigma_i) \quad \text{for each } k \in \mathcal{K}, \underline{s}_k \in [q]^{|k|}. \quad (8)$$

Monomial basis: For the special case of binary variables with $\sigma_i \in \{-1, 1\}$, we can define the monomial basis for any $\mathcal{K} \subset 2^{[p]}$ as

$$g_k(\underline{\sigma}_k) = \prod_{i \in k} \sigma_i \quad \text{for each } k \in \mathcal{K}. \quad (9)$$

When $\mathcal{K} = 2^{[p]}$ both the *centered indicator basis* and the *monomial basis* are complete. However, this choice makes GRISE, as given in (5), clearly intractable. Without any known strong underlying

structure, a natural, and perhaps the only logical choice, is to restrict the so-called *interaction order* to a specified value $L \leq p$ by considering $\mathcal{K} = \{k \in 2^{[p]} \mid |k| \leq L\}$. The complexity of GRISE is driven by the number of terms in the exponent in the objective which is now bounded by $O(p^L)$. A natural hierarchy of basis functions is constructed by starting from $L = 1$, and increasing in small steps as required. We thus obtain increasing representation power at the expense of higher computational cost. This approach is highly effective when the interaction order of the true underlying model is low. However, for models with high interaction order this approach can be computationally expensive, even if the model has significant structure.

3 NeurISE: Neural Interaction Screening Estimator

To deal with higher order models more easily, we use GRISE with a neural net ansatz to represent the partial energy function. A neural net, being a universal function approximator, will eventually cover the space of models as its size is increased and provides a natural alternative to the monomial and centered indicator hierarchies in Section 2.2. But it explores the function space in a different way, and given the ability of neural nets to find patterns in data, it is to be expected that this approach will work better in practice for learning structured models with high interaction order.

3.1 Neural net parameterization of partial energy function

The analysis of GRISE in [30] relies on the linearity of $H(\underline{\sigma})$ in the parameters and the centered property of g_k , none of which is true for a neural net parameterization. Nevertheless, our approach using neural nets attempts to generalize the intuition regarding the zero gradient property of the infinite-sample limit of ISO in (6). Similar to GRISE, we propose a neural network parameterization for one variable u at a time given by approximating the partial energy function H_u in (4) as

$$H_u(\underline{\sigma}) \approx \tilde{H}_u(\underline{\sigma}, w) = \langle \Phi(\sigma_u), \text{NN}_u(\underline{\sigma}_{\setminus u}, w) \rangle = \sum_{s=1}^q \Phi_s(\sigma_u) \text{NN}_u(\underline{\sigma}_{\setminus u}, w)(s), \quad (10)$$

where $\Phi(\sigma_u) = \{\Phi_1(\sigma_u), \dots, \Phi_q(\sigma_u)\}$ and the function $\text{NN}_u(\underline{\sigma}_{\setminus u}, w)$ in (10) is a vector valued function with q outputs. The input to the neural net $(\underline{\sigma}_{\setminus u})$ is the set of all variables except σ_u . We use w to denote the weights of the neural net and they serve the role of the parameters $\underline{\theta}$ in (4). The representation above is automatically centered in σ_u . Moreover, the representation does not lose any generality since the global energy function can always be written as

$$H(\underline{\sigma}) = H_{\setminus u}(\underline{\sigma}_{\setminus u}) + H_u(\underline{\sigma}) = H_{\setminus u}(\underline{\sigma}_{\setminus u}) + \sum_{a=1}^q \Phi_a(\sigma_u) H_{u,a}(\underline{\sigma}_{\setminus u}). \quad (11)$$

The corresponding neural net interaction screening objective (NeurISO) is given by

$$\mathbf{NeurISO:} \quad L_u(w) = \frac{1}{n} \sum_{t=1}^n \exp(-\langle \Phi(\sigma_u^{(t)}), \text{NN}(\underline{\sigma}_{\setminus u}^{(t)}; w) \rangle), \quad \text{for each } u \in [p]. \quad (12)$$

An intuitive justification for NeurISO – a variational argument: Consider the traditional GRISE with a complete set of the *centered indicator basis* defined in (8) with all terms, i.e., order $L = p$. Due to completeness of the basis, optimizing over the parameters $\underline{\theta}$ is equivalent to optimizing over the set of all discrete functions $f : [q]^p \rightarrow \mathbb{R}$ that are centered w.r.t. σ_u . Since GRISE is able to recover the correct energy function using this basis, it follows that the true partial energy function H_u is a *global optimum* of the following variational problem using the infinite-sample ISO:

$$H_u(\underline{\sigma}) = \operatorname{argmin}_{f: [q]^p \rightarrow \mathbb{R}} \mathbb{E}[\exp(-f(\underline{\sigma}))] \quad \text{subject to:} \quad \sum_{\sigma_u} f(\underline{\sigma}) = 0. \quad (13)$$

Since the objective in (13) is convex in f , the partial energy function H_u is the *global optimum* of the problem. When the size of a neural net is sufficiently large, minimizing the NeurISO in (12) is almost equivalent to the variational problem in (13). Although the function \tilde{H}_u is a non-convex function of w , a property similar to the zero gradient property of $\mathcal{S}(\underline{\theta}_u)$ can be shown to hold for L_u in the limit of infinite samples and neural net size when the function space covered by the neural net

is large enough such that there exists a set of weights w such that $H_u = \tilde{H}_u$. In this setting, we can show that one of the minima of L_u corresponds to H_u . The gradient of L_u w.r.t. w can be written as

$$\frac{\partial L_u}{\partial w_j} = -\frac{1}{Z} \sum_{\underline{\sigma}} \langle \Phi(\sigma_u), \frac{\partial \text{NN}(\underline{\sigma}_{\setminus u}; w)}{\partial w_j} \rangle \exp \left(H_u(\underline{\sigma}) - \langle \Phi(\sigma_u), \text{NN}(\underline{\sigma}_{\setminus u}; w) \rangle + H_{\setminus u}(\underline{\sigma}_{\setminus u}) \right).$$

If $H_u(\underline{\sigma}) = \tilde{H}_u(\underline{\sigma}, w)$, for all values of $\underline{\sigma}$, the gradient is zero. We will call the minima for which this condition is satisfied as the *interaction screening minima*.

Since neural networks are universal function approximators [1], we see from the variational problem in (13) that the interaction screening minima are the global optima of L_u over w in the limit of infinite number of samples. This important observation shows that NeurISE always has the capability to learn a neural network representation for the true graphical model from which the samples came from. Even for finite size, this observation motivates the use of SGD or its variants to optimize L_u . The inherent noise in SGD will prevent it from being stuck in any spurious local minima and it will converge more easily to the interaction screening minima. It is further accompanied by its usual perks of parallelizability and the ability to implement using GPUs.

NeurISE as described so far, doesn't learn the full energy function. Instead it gives p neural nets which approximate the partial energy function of each variable in the model. This gives us an approximation for the conditionals of the true model. Let NN_u^* be the fully trained neural net obtained by minimizing L_u . For the true model the conditional probability of a variable conditioned on everything else can be estimated as

$$\mu[\sigma_u | \underline{\sigma}_{\setminus u}] = \frac{\exp(\sum_{a=1}^q \Phi_a(\sigma_u, H_{u,a}(\underline{\sigma}_{\setminus u})))}{\sum_{s=1}^q \exp(\sum_{a=1}^q \Phi_a(s, H_{u,a}(\underline{\sigma}_{\setminus u})))} \approx \hat{\mu}[\sigma_u | \underline{\sigma}_{\setminus u}] = \frac{\exp(\langle \Phi(\sigma_u), \text{NN}_u^*(\underline{\sigma}_{\setminus u}) \rangle)}{\sum_{s=1}^q \exp(\langle \Phi(s), \text{NN}_u^*(\underline{\sigma}_{\setminus u}) \rangle)}. \quad (14)$$

The conditionals can be used to draw samples from the learned model using Gibbs sampling [14].

Remark: Everything in the above discussion carries over to the case of binary models by using

$$H(\underline{\sigma}) = H_{\setminus u}(\underline{\sigma}_{\setminus u}) + \sigma_u H_u(\underline{\sigma}_{\setminus u}) \approx H_{\setminus u}(\underline{\sigma}_{\setminus u}) + \tilde{H}_u(\underline{\sigma}_u) = H_{\setminus u}(\underline{\sigma}_{\setminus u}) + \sigma_u \text{NN}(\underline{\sigma}_{\setminus u}; w), \quad (15)$$

where $\text{NN}(\cdot; w)$ is a scalar valued function.

3.2 Experiments

Now we will test NeurISE on two highly structured graphical models. In our testing we will compare NeurISE to GRISE. These are completely different types of algorithms and finding the right metric to compare them is tricky. GRISE converts the learning problem into a convex optimization problem for which theoretical guarantees can be derived. On the other hand, NeurISE is a non-convex problem but the learning process in this case can be easily parallelized on a GPU using off-the-shelf machine learning libraries. If there are no limitations on the computational power, then both these methods will find the true model eventually. But on real hardware the performance of these will depend on implementation and on the true model being learned. To quantify the hardness of these algorithms in a device independent fashion, we compare the number of free parameters these algorithms optimize over per variable (N_p). Roughly, this number reflects the dimension of the hypothesis space of these algorithms.

We will be using feed forward neural nets with the swish activation function ($\text{swish}(x) = x \cdot \text{sigmoid}(x)$) [25]. We specify the size of a neural net with two numbers, d and w , which will be the number of hidden layers in the model and the number of neurons in each hidden layer respectively. All the nets were trained using the ADAM optimizer [19].

3.2.1 Learning binary models with higher order interactions

We expect NeurISE to work well on models with a high degree of underlying structure even if that model has higher order interactions. GRISE, without any prior information about the structure, will need to use the entire hierarchy described in Section 2.2 to recover the correct model.

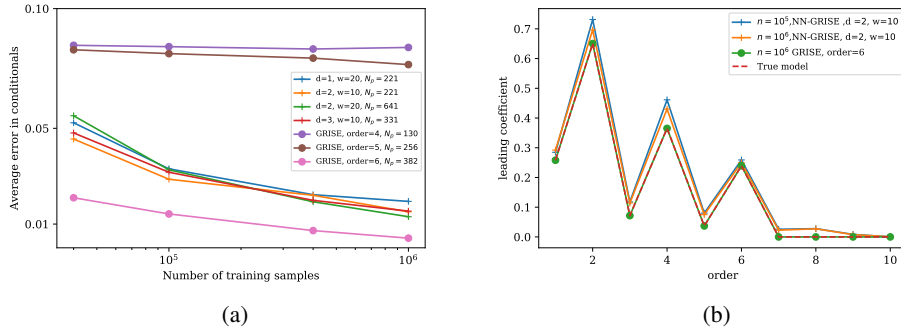


Figure 1: Learning the model given by Eq. (16), with $p = 10$ and $L = 6$. (a) ℓ_1 error in the learned conditionals averaged over all possible inputs. (b) The absolute value of the leading coefficient of the learned model at each order compared to that of the true model.

To demonstrate this, we generate samples from a graphical model with the following energy function,

$$H(\underline{\sigma}) = \sum_{l=1}^L \theta_l^* \sum_{i=1}^{p-l+1} \sigma_i \dots \sigma_{i+l-1}, \quad (16)$$

and learn it using GRISE and NeurISE¹. The hypergraph structure of this model is one dimensional and it has up to L order interactions. We impose an extra symmetry here by choosing the same interaction strength for all terms of the same order. So in effect there are only L parameters to be learned here. But for our experiments the learning algorithms will be unaware of this property and also of the one dimensional nature of the model. First we compute the ℓ_1 error in the learned conditionals averaged over all possible inputs using Eq. (14). We compare the average error in the learned conditionals for a $p = 10$ variable model with $L = 6$ in Fig. 1a. The θ values are chosen from $[-1, 1]$.

We also study our learned model by expanding the learned neural nets in the monomial basis. This can be done for any binary function using standard formulae [24]. If the neural net learns the correct model, the leading coefficients in the monomial expansion at each order should match those of the true model at that order. The absolute values of these coefficients are compared in Fig.1b. Both these metrics are exponentially expensive in p to compute. The small model makes these explicit comparisons possible without resorting to Gibbs sampling.

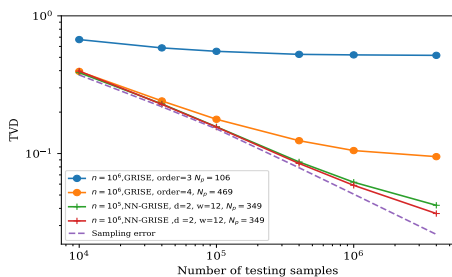


Figure 2: Error in TVD in the learned models when the true model is a 15 variable, sixth order model as given in Eq. (16). The GRISE order is chosen so that it has approximately the same number of free parameters as NeurISE. The x-axis gives the number of samples drawn from the model after learning it.

We see from Fig. 1a that GRISE with all terms up to fifth order ($L = 5$), just one order lower than the true model, fails to learn the model correctly. For this algorithm the number of input samples has little effect on the error in the conditionals. This implies that the candidate models considered by the algorithm are far away from the true model in function space. Including all terms up to fifth order in GRISE requires us to optimize over 256 free parameters. A neural net model comparable to this is the $[d = 2, w = 10]$ model which has 221 free parameters to optimize. We see that this model has better error in comparison to GRISE with similar N_p . Also the error in this case decays as the number of training samples increases, unlike the floor observed in $L=5$ -GRISE. This is an indication that the neural net manages to learn the true model.

Looking at the other neural net models, we see that most of them learn the true model well. The best algorithm according to Fig. 1a is GRISE with sixth order interactions included. This is expected because it has the advantage of having the

¹The code and data for this can be found at <https://github.com/lanl-ansi/NeurISE>.

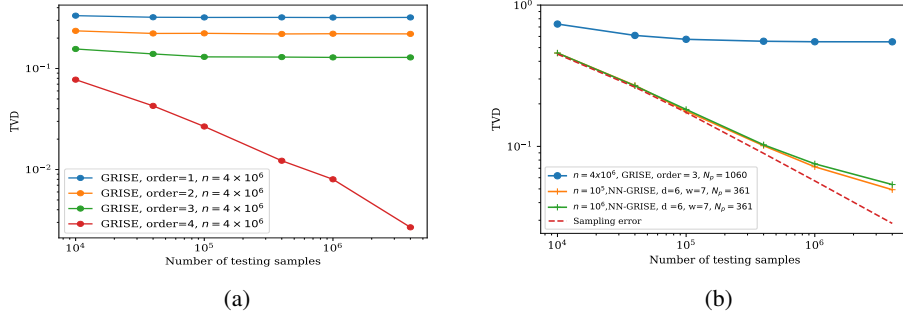


Figure 3: Learning the GHZ state (a) GRISE on the 4 qubit state showing the presence of terms up to the highest order (b) Total variation distance between the distributions sampled from the GHZ state on 7 qubits and those sampled from the learned models.

true model in its hypothesis space. On the other hand, with NeurISE we can only get close to the true model. But the advantage of NeurISE is that it can do this with far fewer parameters than L=6-GRISE, with just 382 parameters.

In Fig. 1b, we see that the neural net learns the coefficients well up to sixth order. But it cannot completely suppress the higher order coefficients. This happens because NeurISE implicitly has higher order polynomials in its hypothesis space. The agreement with the true model improves as the number of training samples increases and the spurious hypotheses are suppressed.

The efficiency of NeurISE over GRISE is obvious for models with a higher number of variables. For larger models we have to resort to sampling from the models and computing the total variation distance (TVD) between the sampled distributions. To set a base line for sampling error we take two independent set of samples from the true model and compare the TVD between them. If the learned model is close to the true model then the TVD between their samples should closely follow this base line. GRISE with sixth order parameters for a 15 variable model is a 3472 variable optimization problem. This was intractable on the hardware used for these experiments. Instead we compare GRISE with up to fourth order interactions ($N_p = 469$) with $[d = 2, w = 12]$ NeurISE ($N_p = 349$). This comparison is given in Fig. 2. We see that NeurISE learns the true model well with fewer number of parameters in comparison to GRISE with a higher N_p , and performs better than GRISE even with fewer training samples.

3.2.2 Learning a $q = 4$ model with permutation symmetry

Now we test NeurISE on graphical models over $\{1, 2, 3, 4\}^p$. Additionally these distributions will also have complete permutation symmetry, i.e. the probability of a string will not change under permutations of that string,

$$\mu(\sigma_1, \sigma_2, \dots, \sigma_p) = \mu(\sigma_{\pi(1)}, \sigma_{\pi(2)}, \dots, \sigma_{\pi(p)}), \quad \forall \pi \in S_p, \quad (17)$$

where S_p is the symmetric group on p elements. Distributions with this symmetry occur naturally in quantum physics. For this specific experiment we will learn the probability distribution obtained by measuring a quantum state called the *GHZ state on p qubits*. We will work with the distribution obtained from the GHZ state by measuring it in a basis known as the *tetrahedral POVM*. The mathematical details of this setup can be found in Ref. [6]. Measuring a p qubit GHZ state in this basis produces a positive distribution on $[4]^p$ which is symmetric under permutations. This means that this distribution can be represented as a Gibbs distribution. Our testing on small systems show the energy function of this distribution has all terms up to order p . (Fig. 3a). Fig. 3b shows the error measured in TVD when learning a GHZ state on 7 qubits. Doing full GRISE in this case is prohibitively expensive ($N_p = 62500$). But NeurISE performs remarkably well with a small neural net ($N_p = 361$).

4 Structure learning with input regularization

In this section we will discuss structure learning with NeurISE, where the focus is to learn the structure of the hypergraph associated with the true model. The ensuing discussion will focus on binary models for simplicity, but the same principle applies for all alphabets.

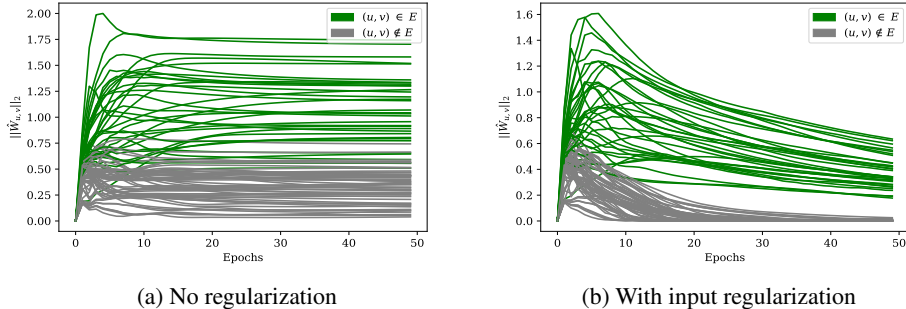


Figure 4: The effect of regularization on the training of input weights. [$p = 10, \alpha = 0.2, \beta = 1.2, d=2, w = 10, n = 4 \times 10^5$].

If NeurISE converges to an interaction screening minima then NN_u^* will contain information about the sites in the neighbourhood of u in the hypergraph of the true model. More precisely, for inputs in $\{1, -1\}^{p-1}$, the output of NN_u^* will be insensitive to the inputs corresponding to sites outside the neighbourhood of u . By looking at which inputs influence the output, we can learn the underlying dependency structure of the graphical model. If a certain input doesn't influence the output, then we expect the input weights connecting that input to the rest of the net to be close to zero. But, NN_u^* is a function whose full domain is \mathbb{R}^{p-1} which we are restricting to $\{1, -1\}^{p-1}$. This restriction is a many to one map in the space of functions, i.e. there are many functions with a continuous domain that can be projected to the same function with a discrete domain. This means that NN_u^* could be a function that depends on all its inputs when its domain is continuous. It could very well have non-zero weights at certain inputs while being not sensitive to those inputs when they take discrete values.

This problem can be fixed in practice by taking two steps. First, at the beginning of training the input weights must be initialized to zero. Secondly, we must regularize the NeurISE loss function with the ℓ_1 norm of only the input weights. Both these steps will ensure that the weights corresponding to the inputs that do not influence the output go to zero.

We test this method on pairwise binary models on random graphs. The energy function here will be $H(\underline{\sigma}) = \sum_{(u,v) \in E} \theta_{u,v}^* \sigma_u \sigma_v$. The random graph is generated by the Erdős-Rényi model [13] and the interaction strengths are chosen uniformly random from an interval $[\alpha, \beta]$. We denote by $\hat{W}_{u,v}$ the array of input weights of NN_u^* that connect the input corresponding to site v to the rest of the network. In Fig. 4, we see the effect regularization and initialization has on $\|\hat{W}_{u,v}\|_2$ while NeurISE is being trained. Regularization forces the non-edge weights to zero and clearly separates them from the edge weights. This means that by plotting a histogram of $\|\hat{W}_{u,v}\|_2$ values at the end of training, we can distinguish between the edges and non edges in the graph. This is demonstrated in Fig. 5, where a 20 variable random graph is reconstructed perfectly from the histogram of trained weights. For a model with higher order interactions, NeurISE will be able to learn neighborhood of each variable. This information can then even be used as a prior in GRISE to reduce its computational cost.

In the case of GRISE there is an exact formula that lets us choose a value for the regularization penalty parameter. The theoretical arguments used to derive that formula do not apply to NeurISE. Yet, the $O(\sqrt{\ln(p)/n})$ formula used for GRISE (Theorem 1, [29]) is seen to be a good rule of thumb for choosing the regularization penalty for NeurISE as well. A low penalty will produce a flat histogram of input weights with no cluster near zero. While a high penalty would force all the input weights to be close to zero. If there are enough samples available for structure learning, then the correct regularization penalty must set the non-edge input weights to zero while keeping the edge input weights at non-zero. Nevertheless, Fig. 4a shows that even if the penalty is too low the input weight histogram will order the edges correctly i.e. the non-edges will have lower weights than the edges. So even in this case there exists a threshold that can separate the edges from the non-edges. The correct regularization penalty makes this threshold more evident in the histogram. As the edges are ordered correctly we can always choose a low threshold if we want to avoid true edges being classified as non-edges by the algorithm. And vice-versa, we can choose a high threshold

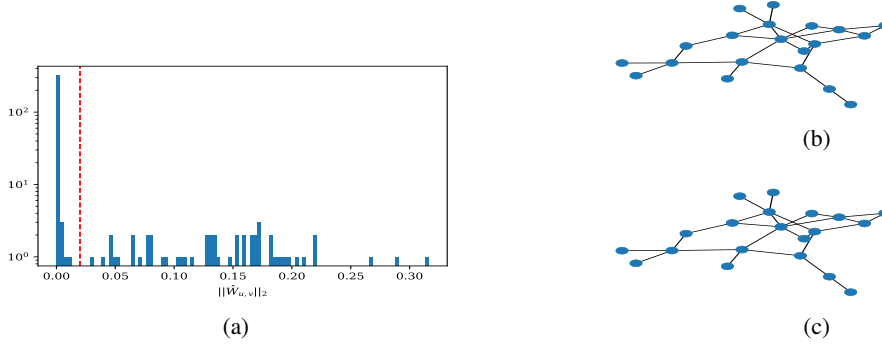


Figure 5: Structure learning on a random graph of average degree of 2.6 [$p = 20$, $\alpha = 0.3$, $\beta = 1.3$, $d=2$, $w = 10$, $n = 4 \times 10^5$] (a) The histogram of $\|\hat{W}_{u,v}\|_2$ after training. The vertical red line is the threshold used to distinguish edges from non edges. (b) Graph of the true model. (c) Graph reconstructed from the histogram.

if we want to avoid non-edges in the true model being classified as edges by the algorithm. More experiments on structure learning and further discussions on choosing this threshold can be found in the supplementary material.

5 Learning the complete energy function with NeurISE

NeurISE as described so far learns the conditionals of the graphical model. At the level of the energy function, the learned model for a particular variable represents the partial energy function of that variable. But for some applications it would be beneficial to have the complete energy function.

Reconstructing the energy function from the partial energies is a non-trivial task. If all the partial energies are compatible, i.e. if they come from the same underlying energy function, then we can expand them in the monomial basis and reconstruct the energy function from the expansion. But this method is computationally expensive. Instead a simple modification to the NeurISE loss function can let us learn the complete energy function directly. We will explain this for the case of binary models, but a similar principle can be used for models with general alphabets as well. The modification to learn the energy function is based on (15) which shows that the partial energy for a variable u can be written as,

$$H_u(\underline{\sigma}) = \sigma_u H_u(\underline{\sigma}_{\setminus u}) = \frac{1}{2} (H(\underline{\sigma}) - H(\underline{\sigma}_{\sim u})), \quad (18)$$

where $\underline{\sigma}_{\sim u}$ is $\underline{\sigma}$ with the variable u flipped in sign. Using a neural net as a candidate for the energy function $H(\underline{\sigma}) \approx \text{NN}(\underline{\sigma}; w)$, we can rewrite the loss in Eq. (3) as

$$L_u(w) = \frac{1}{n} \sum_{t=1}^n \exp \left(\frac{\text{NN}(\underline{\sigma}_{\sim u}; w) - \text{NN}(\underline{\sigma}; w)}{2} \right) \quad (19)$$

To ensure that the trained neural net gives the correct energy function we have to sum up these individual loss functions to construct a single loss function,

$$L(w) = \sum_{u=1}^p L_u(w) = \frac{1}{n} \sum_{u=1}^p \sum_{t=1}^n \exp \left(\frac{\text{NN}(\underline{\sigma}_{\sim u}; w) - \text{NN}(\underline{\sigma}; w)}{2} \right). \quad (20)$$

Just as before, we can show that if the neural net has sufficient expressive power and if $n \rightarrow \infty$, then the global minima of this loss function correspond to the correct energy function. For GRISE this modification is not necessary as it learns directly in the monomial basis. The results of learning a model with this loss function is given in the supplementary material due to space considerations.

Broader impact.

We believe that this work, as presented here, has no direct ethical impact or societal consequences. But, our work paves way for learning higher order graphical models on real world data sets. There

are many unanswered questions about NeurISE that are relevant to such real-world applications. For instance, can any theoretical guarantees be given on the structure learned by NeurISE? Or, can we modify NeurISE to learn a model free of certain biases present in the training data set? We hope to answer some of these questions in the future.

Acknowledgments

We acknowledge support from the Laboratory Directed Research and Development program of Los Alamos National Laboratory under project numbers 20190059DR, 20190195ER, 20190351ER, and 20210078DR.

References

- [1] Andrew R Barron. Universal approximation bounds for superpositions of a sigmoidal function. *IEEE Transactions on Information theory*, 39(3):930–945, 1993.
- [2] Ivona Bezáková, Antonio Blanca, Zongchen Chen, Daniel Stefankovic, and Eric Vigoda. Lower bounds for testing graphical models: Colorings and antiferromagnetic ising models. *Journal of Machine Learning Research*, 21(25):1–62, 2020.
- [3] Bhaswar B Bhattacharya and Sumit Mukherjee. Inference in ising models. *Bernoulli*, 24(1):493–525, 2018.
- [4] Guy Bresler. Efficiently learning Ising models on arbitrary graphs. In *Proceedings of the forty-seventh annual ACM symposium on Theory of computing*, pages 771–782, 2015.
- [5] Stephen G Brush. History of the Lenz-Ising model. *Reviews of modern physics*, 39(4):883, 1967.
- [6] Juan Carrasquilla, Giacomo Torlai, Roger G Melko, and Leandro Aolita. Reconstructing quantum states with generative models. *Nature Machine Intelligence*, 1(3):155–161, 2019.
- [7] Sourav Chatterjee et al. Estimation in spin glasses: A first step. *The Annals of Statistics*, 35(5):1931–1946, 2007.
- [8] C Chow and Cong Liu. Approximating discrete probability distributions with dependence trees. *IEEE transactions on Information Theory*, 14(3):462–467, 1968.
- [9] Yuval Dagan, Constantinos Daskalakis, Nishanth Dikkala, and Anthimos Vardis Kandiros. Estimating ising models from one sample. *arXiv preprint arXiv:2004.09370*, 2020.
- [10] Constantinos Daskalakis, Nishanth Dikkala, and Gautam Kamath. Testing ising models. *IEEE Transactions on Information Theory*, 65(11):6829–6852, 2019.
- [11] Constantinos Daskalakis, Nishanth Dikkala, and Ioannis Panageas. Regression from dependent observations. In *Proceedings of the 51st Annual ACM SIGACT Symposium on Theory of Computing*, pages 881–889, 2019.
- [12] Constantinos Daskalakis, Nishanth Dikkala, and Ioannis Panageas. Logistic-regression with peer-group effects via inference in higher order ising models. *arXiv preprint arXiv:2003.08259*, 2020.
- [13] Paul Erdős and Alfréd Rényi. On the evolution of random graphs. *Publ. Math. Inst. Hung. Acad. Sci*, 5(1):17–60, 1960.
- [14] S. Geman and D. Geman. Stochastic relaxation, Gibbs distributions, and the Bayesian restoration of images. *IEEE Transactions on Pattern Analysis and Machine Intelligence*, PAMI-6(6):721–741, 1984.
- [15] Promit Ghosal, Sumit Mukherjee, et al. Joint estimation of parameters in ising model. *Annals of Statistics*, 48(2):785–810, 2020.
- [16] Linus Hamilton, Frederic Koehler, and Ankur Moitra. Information theoretic properties of markov random fields, and their algorithmic applications. In I. Guyon, U. V. Luxburg, S. Bengio, H. Wallach, R. Fergus, S. Vishwanathan, and R. Garnett, editors, *Advances in Neural Information Processing Systems 30*, pages 2463–2472. 2017.
- [17] Kurt Hornik. Approximation capabilities of multilayer feedforward networks. *Neural networks*, 4(2):251–257, 1991.

- [18] Hilbert J. Kappen and Francisco de Borja Rodríguez. Efficient learning in Boltzmann machines using linear response theory. *Neural Computation*, 10(5):1137–1156, 1998.
- [19] Diederik P Kingma and Jimmy Ba. Adam: A method for stochastic optimization. *arXiv preprint arXiv:1412.6980*, 2014.
- [20] A. Klivans and R. Meka. Learning graphical models using multiplicative weights. In *2017 IEEE 58th Annual Symposium on Foundations of Computer Science (FOCS)*, pages 343–354, Oct 2017.
- [21] Sébastien Lachapelle, Philippe Brouillard, Tristan Deleu, and Simon Lacoste-Julien. Gradient-based neural dag learning. In *International Conference on Learning Representations*, 2019.
- [22] Andrey Y Lokhov, Marc Vuffray, Sidhant Misra, and Michael Chertkov. Optimal structure and parameter learning of Ising models. *Science advances*, 4(3):e1700791, 2018.
- [23] Thierry Mora and William Bialek. Are biological systems poised at criticality? *Journal of Statistical Physics*, 144(2):268–302, 2011.
- [24] Ryan O’Donnell. *Analysis of boolean functions*. Cambridge University Press, 2014.
- [25] Prajit Ramachandran, Barret Zoph, and Quoc V Le. Swish: a self-gated activation function. *arXiv preprint arXiv:1710.05941*, 7, 2017.
- [26] Pradeep Ravikumar, Martin J Wainwright, John D Lafferty, et al. High-dimensional Ising model selection using l_1 -regularized logistic regression. *The Annals of Statistics*, 38(3):1287–1319, 2010.
- [27] Narayana P Santhanam and Martin J Wainwright. Information-theoretic limits of selecting binary graphical models in high dimensions. *IEEE Transactions on Information Theory*, 58(7):4117–4134, 2012.
- [28] Toshiyuki Tanaka. Mean-field theory of Boltzmann machine learning. *Physical Review E*, 58(2):2302, 1998.
- [29] Marc Vuffray, Sidhant Misra, Andrey Lokhov, and Michael Chertkov. Interaction screening: Efficient and sample-optimal learning of Ising models. In *Advances in Neural Information Processing Systems*, pages 2595–2603, 2016.
- [30] Marc Vuffray, Sidhant Misra, and Andrey Y Lokhov. Efficient learning of discrete graphical models. *arXiv preprint arXiv:1902.00600*, 2019.
- [31] Chaohui Wang, Nikos Komodakis, and Nikos Paragios. Markov random field modeling, inference & learning in computer vision & image understanding: A survey. *Computer Vision and Image Understanding*, 117(11):1610–1627, 2013.
- [32] Shanshan Wu, Sujay Sanghavi, and Alexandros G Dimakis. Sparse logistic regression learns all discrete pairwise graphical models. In *Advances in Neural Information Processing Systems*, pages 8071–8081, 2019.

Supplementary Material

This section contains supplementary materials for the paper “Learning of Discrete Graphical Models with Neural Networks”. Here we show results of some more experiments done with NeurISE. Section A has results of learning the Ising model. Section B has more results on structure learning, including learning hypergraphs. Section C has results on learning the full energy function using NeurISE.

A Learning Ising models.

For this experiment we learn Ising models with two body interactions. We take random graphs with an average degree of three and choose the interaction strengths uniformly at random from $[-1,1]$. The Hamiltonian here has the form,

$$H(\underline{\sigma}) = \sum_{i<j} \theta_{ij}^* \sigma_i \sigma_j. \quad (21)$$

This is an adversarial experiment for NeurISE when compared to GRISE. GRISE will learn this model in the second level of its hierarchy with $O(p)$ parameters per optimization. The neural net will have to fit a linear function of its inputs, which it will not be able to do as well as low-degree GRISE. Despite this, NeurISE does a good job of learning the true model, albeit with more number of free parameters when compared to second order GRISE.

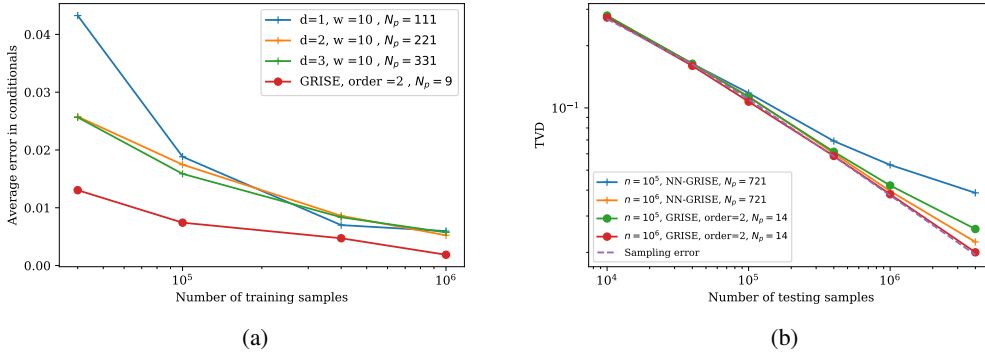


Figure 6: Learning a random Ising model (a) ℓ_1 error in the learned conditionals averaged over all possible inputs for a 10 variable model (b) TVD between samples drawn from the learned models and those drawn from the true model for a 15 variable model. The neural net used here is $[d=3, w=15]$.

B Structure learning with NeurISE.

B.1 Learning hypergraphs

We show that NeurISE can accurately reconstruct the neighbourhood of each variable for a general model with higher order interactions. In Fig 7 we learn the following 15 variable model ²,

$$H(\underline{\sigma}) = \frac{1}{2} \sigma_1 \sigma_3 \sigma_5 \sigma_7 \sigma_9 + \theta_{1,15}^* \sigma_1 \sigma_{15} + \sum_{i=1}^{14} \theta_{i,i+1}^* \sigma_i \sigma_{i+1} \quad (22)$$

The θ^* parameters here are chosen uniformly from $[0.3, 1.3]$. As seen in Fig. 7b, NeurISE can perfectly reconstruct the neighbourhoods of each variables. The fifth order term shows up as clique of size 5 connecting the corresponding variables. Once the neighborhood reconstruction is done, we can use this as a prior in GRISE. This can reduce the number of free parameters in L -order GRISE from $O(p^L)$ to $O(D^L)$, where D is the size of the neighbourhood of the variable being learned.

²Code available at <https://github.com/lan1-ansi/NeurISE>.

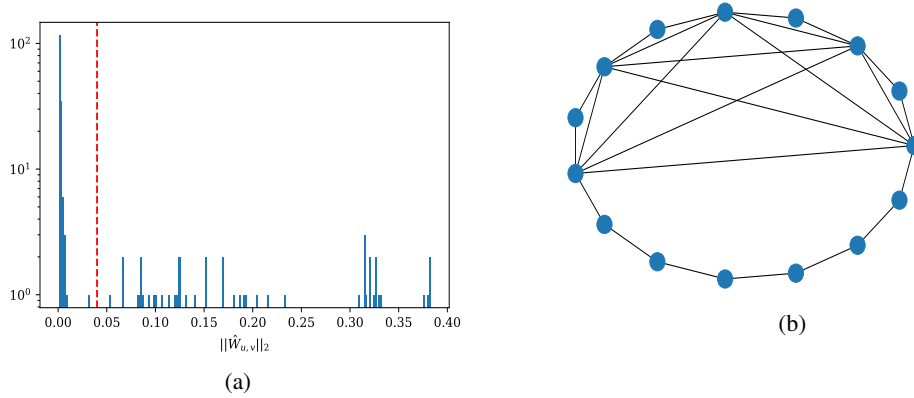


Figure 7: Structure learning on the energy function in Eq. (22) [$p = 15$, $\alpha = 0.3$, $\beta = 1.3$, $d=2$, $w = 15$, $n = 10^6$]. (a) The histogram of $\|\hat{W}_{u,v}\|_2$ after training. The vertical red line is the threshold used to distinguish edges from non edges. (b) Reconstructed graph. The neighbourhood of every variable is learned perfectly

B.2 Learning graphs when the number of samples is too low

The success of structure learning depends on the number of samples used in the algorithm. The number of samples required to perfectly learn the structure depends on the strength of interaction and the degree of the underlying model. This is reflected in the sample complexity lower bound which is exponential in the product of the degree of the graph and the maximum strength of interaction [27]. In particular, learning models with higher degree with a limited number of samples makes distinguishing edges from non-edges more difficult. The histogram of trained inputs weights in this case will be more spread out as seen in Fig. 8a. Despite this there are only a few mis-classified edges in the reconstructed graph. In the histogram these edges usually lie close to the large cluster of weights close to zero. If the threshold line is chosen right after this large cluster most edges and non-edges are classified accurately. GRISE also exhibits a similar behaviour when the number of samples available are inadequate for perfect structure learning [22].

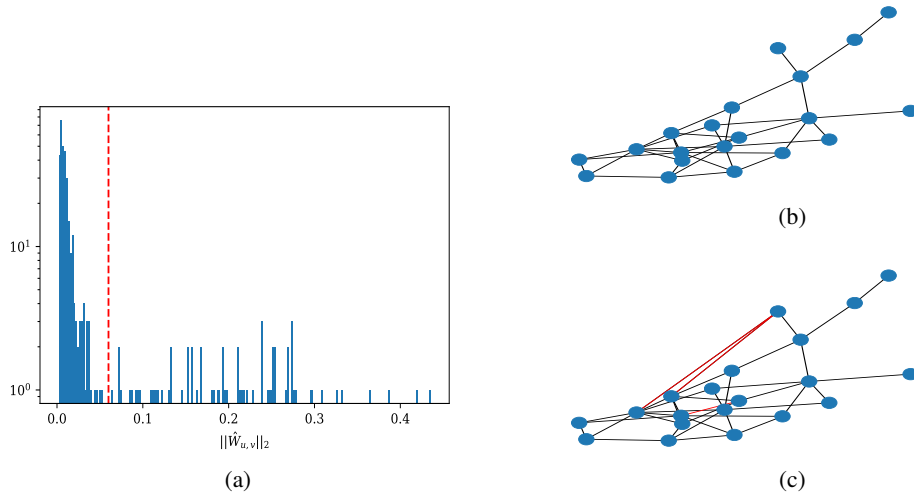
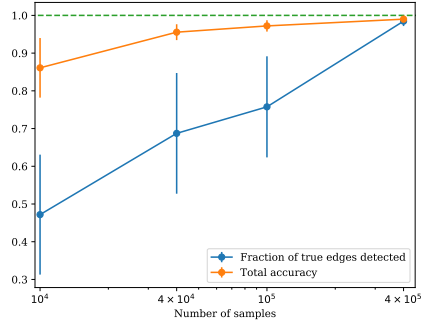


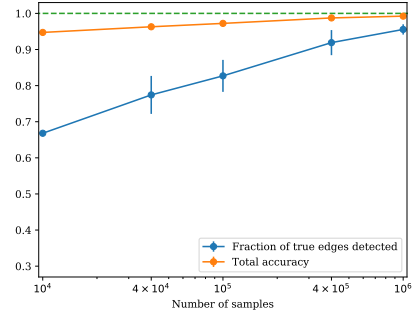
Figure 8: Structure learning on a random graph of average degree of 3.6 [$p = 20$, $\alpha = 0.3$, $\beta = 1.3$, $d=2$, $w = 10$, $n = 10^6$] (a) The histogram of $\|\hat{W}_{u,v}\|_2$ after training. The vertical red line is the threshold used to distinguish edges from non edges. (b) Graph of the true model. (c) Graph reconstructed from the histogram. Mis-classified edges are marked in red.

B.3 Accuracy of structure learning

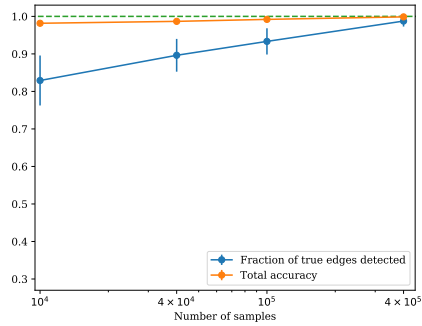
Here we will look at the accuracy of structure learning with NeurISE over randomized experiments.



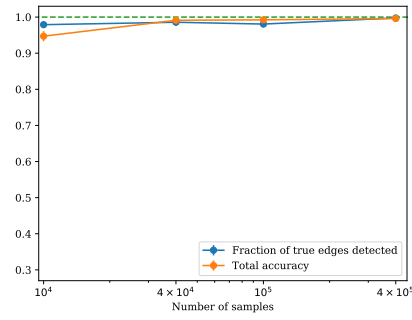
(a) Random second order model with 30 variables, average degree= 3, $d = 2$, $w = 10$.



(b) 20 variable model in Eq.(22) with the fifth order term randomized, average degree = 3, $d = 2$, $w = 20$.



(c) Random third order model with 30 variables, average degree = 2, $d = 2$, $w = 10$



(d) Random fourth order model with 30 variables, average degree = 2, $d = 2$, $w = 10$

Figure 9: Accuracy of structure learning over randomized experiments with confidence intervals. For every model we take, $[\alpha, \beta] = [0.3, 1.3]$. Every data point is result of 20 randomized experiments. The “Total Accuracy” here refers to the accuracy of the algorithm for learning both edges and non-edges in the graph. The average degree of each hypergraph is the average number of neighbours of each node in the hypergraph

The results of structure learning for various classes of models is plotted in Fig.9. Each data point in these plots is a result of 20 randomized experiments. The thresholds for structure learning were chosen automatically by constructing the distribution of input weights and using an outlier detection method to isolate the weights clustered around zero. The edges that were a fraction of the standard deviation away from the mean of the distribution were labelled as edges. The value of this fraction is a fixed value for each of the four experiments in Fig.9. This is fixed first by running a few test experiments and inspecting the histograms of their input weights. The other hyper parameters for learning are also fixed in this fashion. In general, visual inspection of the histogram gives a better value for the threshold. But this is impractical if one has to run many randomized experiments. The method based on the standard deviation of the histogram automates the structure learning process.

Systematically, these experiments show the difference of the neural network hierarchy from the polynomial hierarchy. The sample complexity of learning a neural net representation of a random fourth order model is much smaller than that of learning a random second order model or a random third order. The neural net can learn a random fourth order order with higher accuracy consistently. On the other hand, using the polynomial hierarchy would have made the learning of the lower order models easier. From these results, we also see that structure learning accuracy gets worse with the average degree of the true model. This behavior is consistent with the known lower bounds on the sample complexity of structure learning

These experiments also show that NeurISE has no problem finding the minima corresponding to the true model even when the number of samples is finite.

C Results of learning the energy function with NeurISE.

In this section we will look at the results of learning the complete energy function using NeurISE by training it with the loss function given in Eq. (20). We will look at the results of using this loss on the Energy function in Eq. (16). Since we have the neural net representation for the full energy function we will compute the average loss in the energy function rather than in the conditionals. This comparison for a 10 variable model is given in Fig. 10a. We also compute the TVD between sampled distributions for the 15 variable model in Fig. 10b. The samples are now generated from the neural net using exact sampling rather than Gibbs sampling. This would have been intractable with neural nets approximations of the partial energy functions.

GRISE directly learns in the monomial basis, so the total energy function can be approximated by appropriately averaging the terms in the partial energy function. But this requires p separate optimizations and increases the N_p count of learning the energy function. To make the comparison with NeurISE more fair, instead we compute the N_p value of L -order GRISE as $\sum_{k=1}^L \binom{p}{k}$. This is just the total number of independent parameters in a L -order energy function with p variables.

From Fig. 10, we see that NeurISE learns the energy function well with less N_p . Notice that the neural nets used here are larger in size than that used in learning the partial energies. But here a single neural net learns the complete model, while in the other case we had p separate nets learning the model.

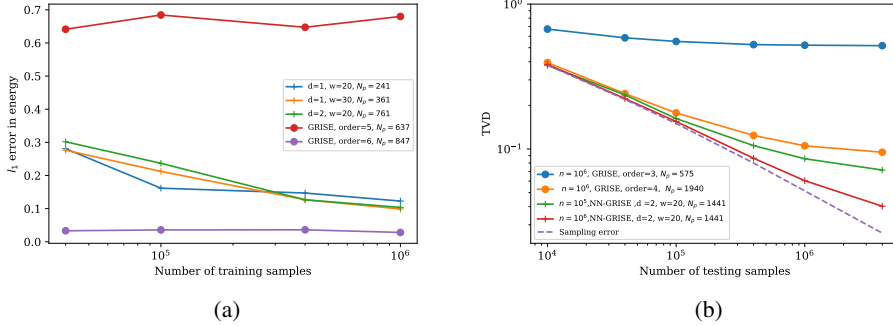


Figure 10: Learning the full energy function of the model in Eq. (16) (a) Average ℓ_1 error in energy for a 10 variable model (b) TVD between samples drawn from the learned models and those drawn from the true model for a 15 variable model